Electronic structures, total energies, and optical properties of α-rhombohedral B_{12} and α-tetragonal B_{50} crystals

Dong Li, Young-Nian Xu, and W. Y. Ching
Department of Physics, University of Missouri–Kansas City, Kansas City, Missouri 64110
(Received 29 July 1991)

The band structures of α-rhombohedral B_{12} (α-r-B_{12}) and α-tetragonal B_{50} (α-t-B_{50}) crystals have been calculated by means of the first-principles orthogonalized linear combination of atomic orbitals method. It is shown that α-r-B_{12} is a semiconductor with an indirect band gap of 1.70 eV and α-t-B_{50} is a metal with a semiconductorlike band structure near the Fermi level. The intra-icosahedral and inter-icosahedral bondings in these two crystals are elucidated by resolving the density of states into various partial components, and by studying the valence-charge-density distributions. There is strong evidence for weak three-center bonding in the B crystals, but the traditional view regarding the bonding pattern in icosahedral B_{12} may be oversimplified. The total energies of α-r-B_{12} and α-t-B_{50} are calculated as a function of crystal volumes without change in the symmetry of the crystals. The equilibrium volume, the bulk moduli, and the cohesive energies obtained are in good agreement with available experimental data and some other recent calculations. Using the wave functions obtained from the band-structure calculation, the frequency-dependent interband optical conductivities in α-r-B_{12} and α-t-B_{50} crystals are also calculated. The real and imaginary parts of the dielectric-function curve are shown as a function of photon energy up to 40 eV for α-r-B_{12} and up to 10 eV for α-t-B_{50}. They are significant differences in the optical properties of these two crystals because of the different nature of the band structures. For α-r-B_{12}, a large plasmon excitation at 31 eV is predicted.

I. INTRODUCTION

Boron is one of the few elements that assumes complex crystal forms in its elemental form. Polymorphism in boron is itself a vast field of scientific endeavor. Boron and B-rich compounds have been subjected to increasing studies because of their many unique combinations of properties, such as high melting temperature, extreme hardness and lightness, unique transport and mechanical properties, etc.[1] Boron exists in three main crystalline forms, the α-rhombohedral B_{12} (α-r-B_{12}), the α-tetragonal B_{50} (α-t-B_{50}), and the β-rhombohedral B_{105}. At higher temperatures (>1500 K), β-tetragonal B_{192} and an orthorhombic form of B are also believed to exist.[2] The main structural unit in these crystals is a near-perfect icosahedral B_{12} molecule. Different crystal forms differ in the ways the icosahedra are linked to form the three-dimensional network.[2] Because of the icosahedral symmetry and the fact that the B atom has three valence electrons in four available orbitals, the actual bonding in B crystals and the resultant electronic structures has been a subject of major interest for many years.[1,2]

There have been several theoretical calculations on the electronic structures of the simplest form of B crystal α-r-B_{12}, and the related carbide $B_{12}C_3$ with a similar structure.[3–9] Only very recently, Lee, Bylander, and Kleinman (LBK) performed a fully self-consistent local-density calculation on α-r-B_{12} using the pseudopotential method.[6] Bullett also studied both α-t-B_{50} and β-r-B_{105} in addition to α-r-B_{12}, using a simplified linear combination of atomic orbitals (LCAO) method with a two-center approximation.[4] Recently, Mailhiot, Grant, and McMahan explored the other possible forms of B at high pressure using total-energy local-density calculations.[8]

In this paper, we report a detailed study of the electronic properties of α-r-B_{12} and α-t-B_{50}, using the self-consistent orthogonalized linear combination of atomic orbitals (OLCAO) method. Our results include the band structures, the density of states (DOS), the charge distribution and bonding pattern, the total-energy calculation, and the linear optical properties. We find α-r-B_{12} to be a semiconductor while α-t-B_{50} is a metal. The different nature of the band structure has resulted in fundamentally different optical properties of these two crystals. The possible reason for metallization in α-t-B_{50} and its stability as inferred from the total-energy calculation is discussed in the context of its unusual structure.

The organization of the rest of the paper is as follows. In the next section, the crystal structures of α-r-B_{12} and α-t-B_{50} are discussed in considerable detail. This is followed by a brief outline of the method of calculation. The electronic-structure results of α-r-B_{12} and α-t-B_{50} are presented in Secs. IV and V, respectively. The results on the total-energy calculation and optical properties are presented in Secs. VI and VII. The final section is devoted to a brief summary and some conclusions.

II. CRYSTAL STRUCTURES

The crystal structure of α-r-B_{12} was determined by McCarty *et al.*[10] and also by Decker and Kasper.[11] The rhombohedral cell has a lattice constant $a=5.304$ Å and angle $\beta=58.13°$. The basic structure in the unit cell is a single B_{12} icosahedron which is linked to other icosahed-

rons in the adjacent cells. Each icosahedron is slightly distorted by the Jahn-Teller effect, reducing its symmetry from Ih to D_{3d}. The rhombohedral cell is equivalent to a hexagonal cell with a cell volume three times as large. The crystal structure for α-r-B_{12} in the basal plane of the hexagonal cell perpendicular to the threefold axis is sketched in Fig. 1(a). We have followed Ref. 2 in labeling the atoms on the B_{12} icosahedron as either equatorial (e,e^*) or rhombohedral (t,t^*). Each B atom is linked to five intra-icosahedral atoms and one or two other inter-icosahedral B atoms. It should be noted that in α-r-B_{12}, a perfect pentagonal polyhedron bonding is not attained because the intericosahedral bonding is not along the five-fold axis of symmetry. The triangular configuration on the face of the icosahedron and that between three icosahedrons in the basal plane of Fig. 1(a) is instrumental to the formation of the three-center bonds in B and B-rich compounds.[2]

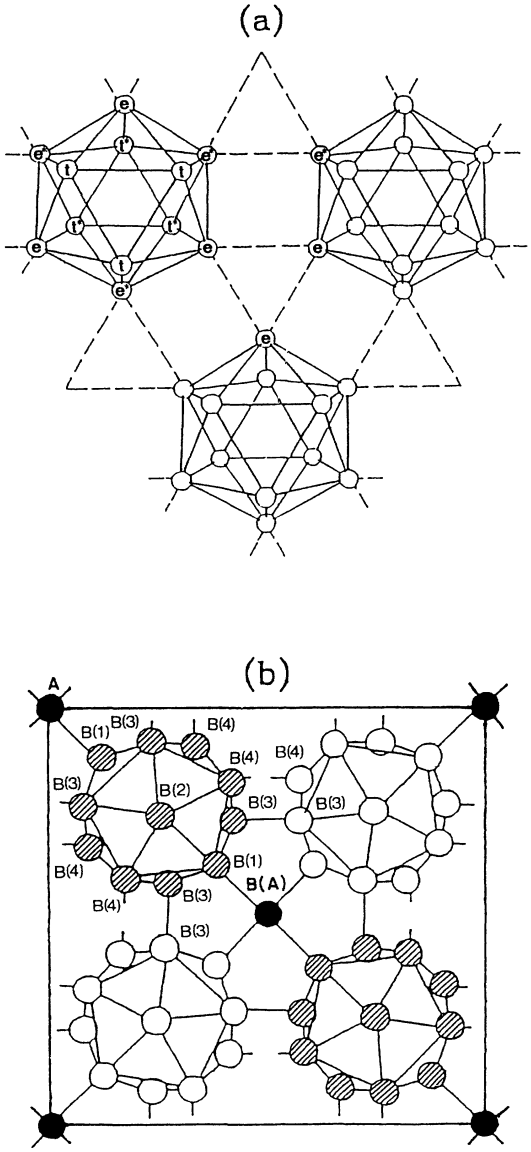

FIG. 1. Crystal structure sketches of (a) α-rhombohedral B_{12} and (b) α-tetragonal B_{50}.

The single-crystal α-t-B crystal was obtained by Laubengayer *et al.*,[12] showing the material to be hard, black, and with a metallic luster. The crystal structure of α-t-B_{50} was proposed by Hoard *et al.*[13,14] The tetragonal cell has lattice parameters $a=8.75$ Å and $c=5.06$ Å and contains four B_{12} icosahedrons and two isolated fourfold-bonded B atoms as shown in the sketch in Fig. 1(b). It is assumed that the icosahedron in α-t-B_{50} is perfect with an intra-icosahedral B-B bond of 1.780 Å. Depending on their connection to B atoms in other icosahedrons or to the isolated central boron atoms (labeled as type A), the twelve B atoms in the four icosahedrons can be divided into four types: B(1), B(2), B(3), and B(4). Each of the B atoms on the icosahedron links to only *one* other boron atom outside the icosahedron, resulting in a lower coordination number for boron atoms in α-t-B_{50} than in α-t-B_{12}. The two B(1) atoms are linked to atoms with a short bond length of 1.658 Å. The two B(2) atoms link to other B(2) atoms in the adjacent cells along the vertical direction. There are four B(3) and four B(4) types of atoms, each of them bonded to other B(3) and B(4) atoms in the adjacent icosahedrons with bond lengths of 1.716 and 1.960 Å, respectively. Thus the B(4)-B(4) separation is significantly larger than other B-B separations. There are large open areas surrounded by B(3) and B(4) atoms. The fourfold type-A B atoms are unique in linking the icosahedrons together to form a three-dimensional network. The bonding pattern of type-A B atoms is a major point of interest.

There are other more complicated forms of boron in β-r-B_{105} (Refs. 15 and 16) and β-t-B_{192} (Ref. 17) and even an (unconfirmed) orthorhombic boron.[18] These structures will not be discussed in the present paper.

The crystal structure information and the interatomic distances for both α-r-B_{12} and α-t-B_{50} are summarized in Table I.

III. COMPUTATIONAL METHOD

The first-principles OLCAO method in the local-density approximation for electronic-structure determination, total-energy calculation, and optical-property studies of crystals has been described in detail.[19] The method is particularly effective in studying crystals with complex structures and low symmetries. We shall only briefly outline the steps of our calculation that are relevant to the present study. The basis functions consist of linear combinations of atomic B 1s, 2s, 2p, 3s, and 3p orbitals, which are expanded as a sum of Gaussian-type orbitals with decaying exponents ranging from 50 000 to 0.15. The potential and charge-density functions are also cast as a sum of atom-centered Gaussian functionals which are numerically fitted to the calculated charge densities. We have adopted a set of 14 Gaussians per site with exponentials ranging from 0.1 to 100 000. The accuracy of the calculation depends very sensitively on the accuracy of the charge-density fit. In the present calculation, we have achieved an accuracy of limiting the fitting error to no more than 0.001 (0.018) electron per valence

electron in α-r-B_{12} (α-t-B_{50}). In the self-consistent iteration, a total of 6 (6) special **k** points in an irreducible portion of the Brillouin zone (BZ) were used for α-r-B_{12} (α-t-B_{50}), while in the final calculation, secular equations were solved at 110 and 18 regularly spaced **k** points for α-r-B_{12} and α-t-B_{50}, respectively. The energy eigenvalues and wave functions at these **k** points were used for the BZ integration to obtain the DOS and also the optical spectra. For the total-energy calculation, we have assumed that the symmetry of the crystal remains the same, i.e., only the lattice constant was scaled to obtain total energy E as a function of volume V. Based on the calculated E vs V data points, the static properties for α-r-B_{12} and α-t-B_{50} were obtained by fitting the data to

TABLE I. Crystal and calculated electronic structures of α-rhombohedral B_{12} and α-tetragonal B_{50}.

	α-r-B_{12}	α-t-B_{50}
Lattice constant (Å)	$a=5.034$ $\beta=58.13°$	$a=8.75$ $c=5.06$
Density (g/cm^3)	2.50	2.32
Space group	$R\bar{3}m$	$P4_2/nnm$
B-B bond length (Å)		
intra-icosahedral	1.740(6) (t-t),(t^*-t^*) 1.783(12) (t-e),(t^*-e^*) 1.794(6) (t-e^*),(t^*-e) 1.772(6) (e-e^*)	1.780(12)
intericosahedral	1.669(6) (t-t^*) 2.003(12) (e-e),(e^*-e^*)	1.658(8) [B(1)-B(A)] 1.673(8) [B(2)-B(2)] 1.716(12) [B(3)-B(3)] 1.960(12) [B(4)-B(4)]
Band gap (eV)		
indirect	1.70 ($Z\rightarrow\Gamma$)	
direct	2.17 (Γ) 4.12 (X) 2.79 (Z) 3.53 (A) 4.12 (D)	2.16 (Γ) 3.20 (X) 3.95 (S) 2.91 (Z)
expt.	1.9[a]	
other calculations (indirect)	1.43[b] 1.70[c]	
Bandwidths (eV)		
upper VB	10.00	10.67 (occupied) 1.37 (above E_F)
middle VB	2.57	2.03
lower VB	0.82	0.33
Effective mass (electron)		
CB edge	0.21 (ΓX) 1.10 (ΓZ) 0.56 (ΓD) 0.58 (ΓA)	
VB edge	−0.21 (ZA) −1.63 ($Z\Gamma$) −0.36 (ΓD) −0.30 (ΓA)	

[a]Reference 21.
[b]Reference 7.
[c]Reference 4.

Murnaghan's equation of state.[20] For the optical calculation, the real part of the frequency-dependent interband optical conductivity $\sigma(\omega)$ was evaluated first in the random-phase approximation with all the transition matrix elements fully included.[19] From the $\sigma(\omega)$ curve, the real and the imaginary parts of the dielectric function, $\epsilon_1(\omega), \epsilon_2(\omega)$, and the electron energy-loss function (ELF) can be extracted.[19]

IV. ELECTRONIC STRUCTURE OF α-RHOMBOHEDRAL B_{12}

The calculated band structure of α-r-B_{12} is shown in Fig. 2. This crystal is shown to be a semiconductor with an indirect band gap of 1.70 eV. The top of the valence band (VB) is at Z and the bottom of the conduction band (CB) is at Γ. This band-gap value is in good agreement with the value of 1.8 eV deduced from the optical measurement of Horn.[21] The pseudopotential calculation of LBK (Ref. 7) gave an indirect band gap of 1.43 eV, while an earlier calculation by Bullett[4] also gave a band gap of about 1.70 eV. The difference in the band-gap value between the present calculation and that of Ref. 7 may be due to the different types of basis functions used, and to a lesser extent, to the different exchange-correlation forms of the potential employed. It is conceivable that further argumentation of the basis set with single Gaussians (to increase the variational freedom) may reduce our calculated gap by about 0.05–0.10 eV.

The effective-mass components along the symmetry lines at both the CB and VB edges have been evaluated and are listed in Table I. Along certain directions, both the hole and electron effective-mass components can be quite small. For example, m_h^*/m along ZA is -0.21 and m_e^*/m along ΓX is 0.21. The small effective-mass component in α-r-B_{12} is consistent with its relatively high hole mobility (in excess of 100 $cm^2/V\,s$ at room temperature).[22]

The DOS and the orbital-resolved partial DOS (PDOS) are shown in Fig. 3. The VB has three segments with a total width of 16.9 eV. The upper VB containing 28 electrons is 10 eV wide and is predominantly composed of B $2p$ states. A deep dip at -5.0 eV separates the upper VB into two regions with 12 electrons in the lower portion and 16 electrons in the upper portion. The middle VB contains 6 electrons and is only 2.5 eV wide with a mixed $2s$ and $2p$ character. The lowest VB of width 0.9 eV is derived from a single band of mostly $2s$ character. The orbital-resolved PDOS show substantial hybridization between B $2s$ and B $2p$ states in all three VB regions.

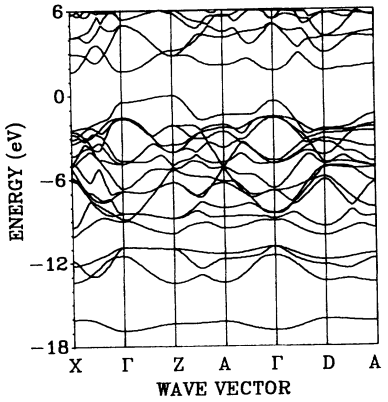

FIG. 2. Calculated band structure of α-r-B_{12}. The zero of energy is at the top of the VB.

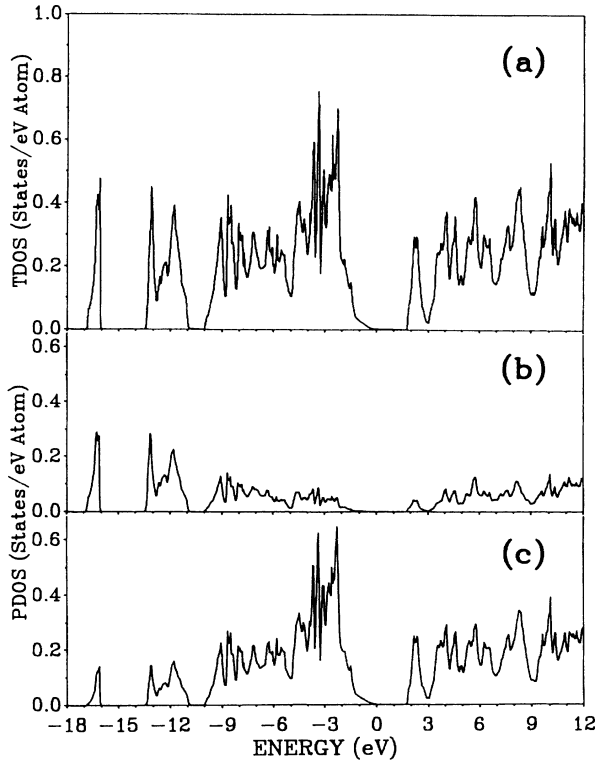

FIG. 3. DOS of α-r-B_{12} (a) total (TDOS); (b) PDOS, B $2s$; (c) PDOS B $2p$.

The valence charge distribution in α-r-B_{12} on three independent icosahedral faces is shown in Fig. 4. The dis-

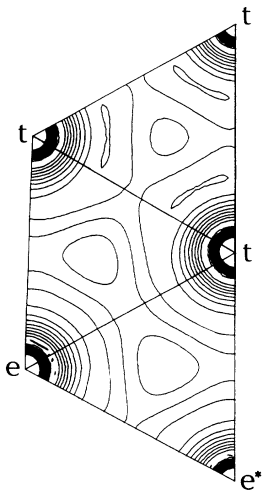

FIG. 4. Charge-density contour on three triangular faces of the icosahedron in α-r-B_{12}. The minimum of the contour is 0.01 and the maximum is 0.25 in intervals of 0.005 [in units of electrons/(a.u.)^3].

tribution of charge on the rectangular and the triangular intericosahedral regions (see Fig. 1) are shown in Figs. 5 and 6, respectively. These charge-density distributions are very similar to the work of Ref. 6 and are also consistent with the x-ray-diffraction measurement of Morosin *et al.*[23] The charge maps show a tendency to form a weak three-center bond on the triangular faces and a weak covalent bond between icosahedrons. The charge contours indicate that the bonding outside the icosahedron is of the same strength as those on the icosahedron. Hence α-r-B_{12} cannot be viewed as a molecular crystal with the icosahedral units bonded by weak van der Waal forces. To see more clearly the nature of the three-center bond, we show the valence charge density in α-r-B_{12} along a B-B direction (t to t) and the three-dimensional charge-density surface on one of the triangular faces of the B_{12} icosahedron (t-t-t) in Figs. 7(a) and 7(b), respectively. There appears to be a weak covalent bond between the B atoms with a very shallow minimum in the middle. There is a charge minimum [0.073 electron/(a.u.)^3] at a distance of 0.21 Å and a double maxima [0.1147 electron/(a.u.)^3] at a distance of 0.56 Å from the boron center. The shallow minimum at the center is only 0.011 electron/(a.u.)^3 below the maxima. The three-dimensional plot of Fig. 7(b) shows some evidence for a weak three-center bond, since there is a considerable charge buildup toward the center of the triangular face.

The formation of three-center bonds in α-r-B_{12} crystal has been attributed to α-r-B_{12} being an electron-deficient system. Longuet-Higgins and Roberts,[24] based on the symmetry-adapted molecular-orbital analysis, argued that there were 13 intra-icosahedral bonding orbitals which account for 26 of the 36 valence electrons in the B_{12} cluster. The remaining 10 electrons were used up in the intericosahedral bonding, 6 for the two-center bonds and 4 for the three-center bonds. This accounts for all the valence electrons in α-r-B_{12}, thus resulting in an insulator band structure.[1] However, the band structure and the DOS in Figs. 2 and 3, and the charge-density plots in Figs. 4–7, indicate that such an argument is grossly oversimplified for the following reasons. (1) The lowest single band in α-r-B_{12} shows a kind of collective bonding involving all 12 atoms in the icosahedron although inspection of eigenvectors shows the predominating contribution from the 2s orbital of the 6 equatorial (e,e^*) boron atoms. (2) The division of the VB DOS into three separate regions containing distinctively 2, 6, and 28 (12 below and 16 above the dip) electrons is incompatible with the notion of 13 intra-icosahedral bonding orbitals. (3) there is a substantial hybridization between s and p orbitals in all three regions. (4) The formation of three-center bonds in the triangular face and weak two-center bonds between two different icosahedrons is only a qualitative description incapable of assigning a specific num-

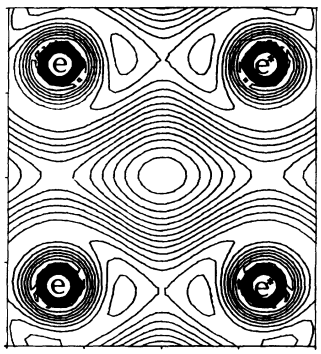

FIG. 5. Charge-density contour in the intra-icosahedral bonding region containing the e-e^*-e^*-e plane [see Fig. 1(b)]. The units of the contour are the same as in Fig. 4.

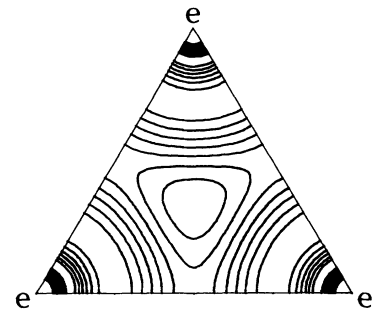

FIG. 6. Charge-density contour in the intra-icosahedral bonding region containing the three center t-t-t B atoms. The units of contour are the same as in Fig. 4.

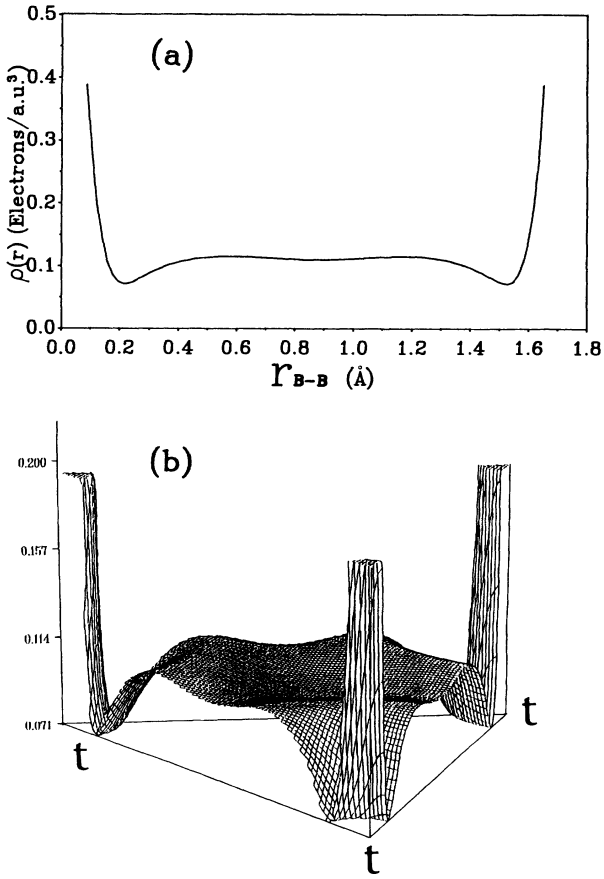

FIG. 7. (a) Charge-density along a B-B bond; (b) Three-dimensional charge surface of the t-t-t face in Fig. 4.

ber (or fraction of it) to the bonds. In other words, the true bonding picture in α-r-B_{12} requires a rigorous quantum-mechanical calculation and cannot be elucidated by a simple molecular-orbital analysis.

V. ELECTRONIC STRUCTURE OF α-TETRAGONAL B_{50}

The calculated band structure for α-t-B_{50} is shown in Fig. 8. It is clear that α-t-B_{50} is a metal with a Fermi surface. The bands are very flat with large effective masses. There is also a significant gap of about 2.16 eV above the top of the VB (metallic band), which is only 1.37 eV from the Fermi level. The electronic structure resembles that of the $YBa_2Cu_3O_7$ superconductor in which an intrinsic hole population exists above the Fermi level at what looks like a semiconductorlike band structure.[25,26] In the case of α-t-B_{50}, this intrinsic hole region can accommodate 10 electrons per unit cell, compared to 4 in the $YBa_2Cu_3O_7$ superconductor. This deficiency of 10 electrons in α-t-B_{50} in forming a perfect normal insulator band structure was used as the basis for the argument that α-t-B_{50} is unstable. Perhaps electron-rich elements must be present in the open interstitial regions in order to stabilize the α-tetragonal structure,[2] such as in the case of $B_{48}B_2C_2$ (Ref. 27) or $B_{48}B_2N_2$ (Ref. 28) crystals. A similar type of band structure in the $YBa_2Cu_3O_7$ and in other high-T_c superconductors implies that this may not be the case after all.

The total DOS and atom-resolved PDOS for α-t-B_{50} are shown in Figs. 9 and 10, respectively. The total DOS, like those in α-r-B_{12}, consists of lower, middle, and upper segments, each of which contains 8, 24, and 128 electrons. For the upper VB, there is again a deep dip at -6 eV with 44 electrons below and 74 electrons above. The main differences in the electronic structure with α-r-B_{12} are the following. (1) The upper VB has an intrinsic hole population of 10 holes resulting in a metallic Fermi surface discussed above. (2) The top VB width in α-t-B_{50} has been increased to 12.0 eV (including the unoccupied hole region) while the lower VB width has been deceased to 0.33 eV, and the middle VB width is slightly decreased to 2.03 eV. (3) The band at the top of the VB is much flatter

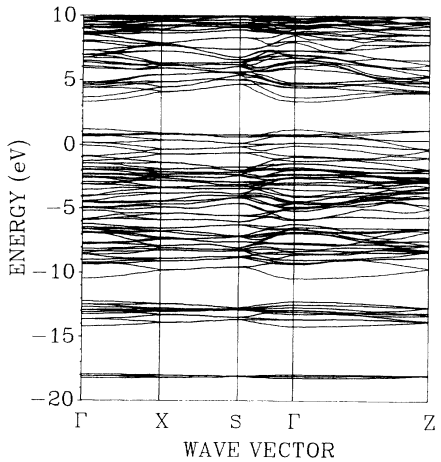

FIG. 8. Band structure of α-t-B_{50}. The zero of energy is at the Fermi level.

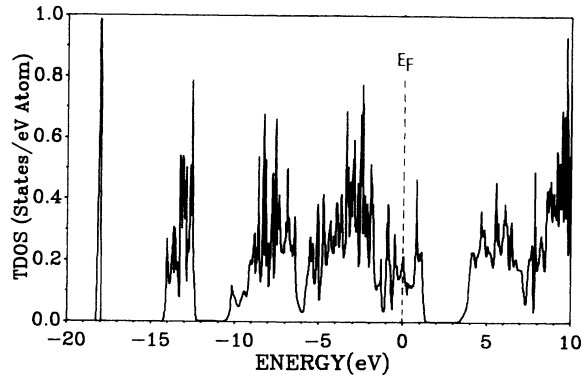

FIG. 9. Total DOS (TDOS) of α-t-B_{50}. The zero of energy is at the Fermi level.

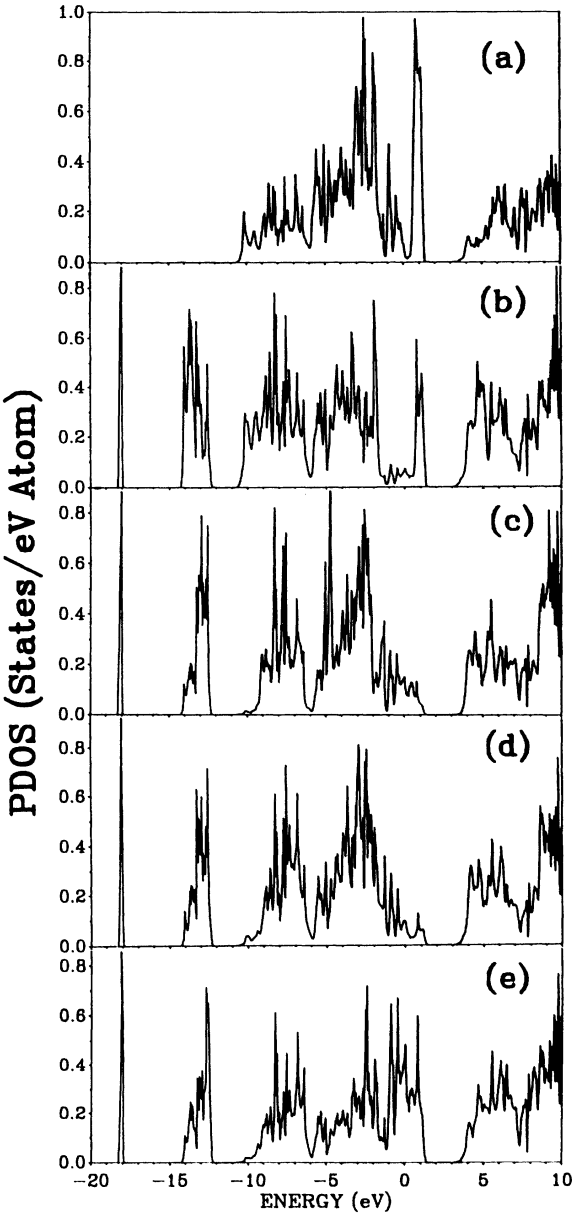

FIG. 10. Partial DOS of α-t-B_{50}: (a) B(A); (b) B(1); (c) B(2); (d) B(3); (e) B(4).

in α-t-B_{50} than in α-r-B_{12}, implying a large hole effective mass in α-t-B_{50}. (4) There are also considerable differences in the structures in the upper and middle VB DOS, and in the CB DOS. These differences in the bandwidths and the band gaps are summarized in Table I.

In order to trace the origin of metallization in α-t-B_{50} in relation to its structure, we resolve the total DOS into partial components according to five different types of B atoms [type-A B, B(1), B(2), B(3), and B(4)] as discussed in Sec. II. The most conspicuous feature is the large narrow peak at the top of the VB for the type-A B and B(1) atoms, indicating a very localized bonding orbital from these two atoms because of its fourfold coordination of A. Note also that A-type atoms are not involved in any states below 10 eV which are exclusively from intra-icosahedral bonding. Next, the B(4) atoms show significant contribution to the DOS in the intrinsic hole region, and this could be due to the relatively large interatomic bonds of 1.960 Å between B(4) atoms of different icosahedrons.

The charge-density contours on the planes involving intericosahedral bonding in α-t-B_{50} are shown in Figs. 11, 12, and 13 for specific planes containing B(1)-B(A)-B(1)′, B(1)-B(3)-B(3)′, and B(4)-B(4)-B(4)′ atoms (here a prime means that the atom is at an adjacent icosahedron). Also

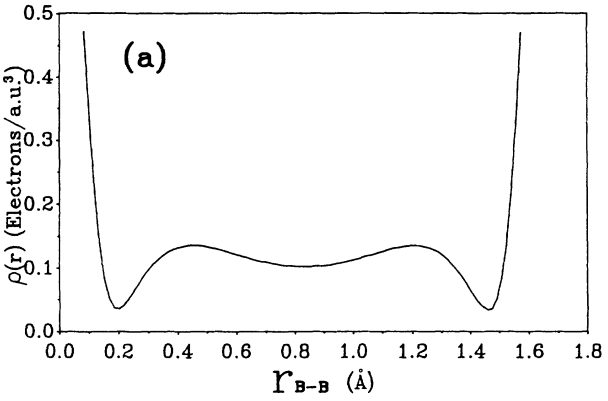

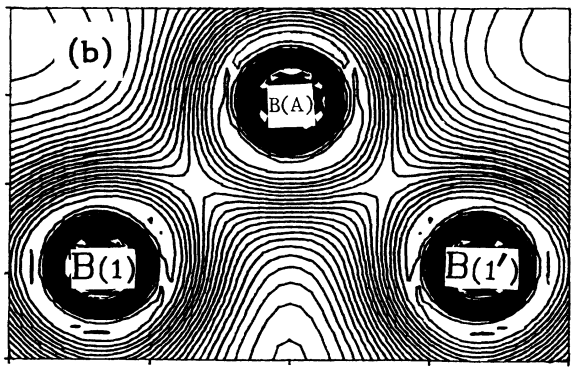

FIG. 11. (a) Charge density along the B(1) to type-A B atom showing strong covalent bonding. (b) Charge-density contour in α-t-B_{50} on a plane containing B(A)-B(1)-B(1)′ atoms [see Fig. 2(b)]. The units of the contour are the same as in Fig. 4.

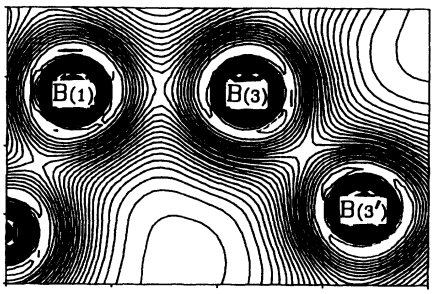

FIG. 12. Charge-density contour in α-t-B_{50} in a plane containing B(1)-B(3)-B(3)′ atoms [see Fig. 2(b)]. The units of the contour are the same as in Fig. 4.

shown in Fig. 11(a) is the bond charge from B(1) to the A atom. These figures show strong covalent bonding between intra-icosahedral B atoms and also with the isolated A-type atoms. It becomes clear, therefore, that the metallization of α-t-B_{50} is mainly due to the presence of low-coordination A-type atoms and also the low-coordination number for intericosahedral bonding.

VI. TOTAL-ENERGY CALCULATION

It has been shown that the OLCAO method is capable of giving very accurate ground-state and bulk-phase-transformation properties via total-energy calculations.[19] Satisfactory total-energy results were obtained for AlN,[29] different phases of Si,[30] and BN crystals in cubic, hexagonal, and wurtzite forms.[31] The total energies of α-r-B_{12} and α-t-B_{50} as a function of volume have been calculated by the OLCAO method. In these calculations, the symmetry of the crystals is not reduced. It is not clear whether this is a good approximation for α-t-B_{50}, since one would tend to believe that the atoms in the icosahedron will be more rigidly bonded than those outside it. Nevertheless, we assume this is the case. The calculated total-energy data at different volumes are fitted to the Murnaghan's equation of state,[18] and the resulting curves for α-r-B_{12} and α-t-B_{50} are shown in Fig. 14(a). The calculated equilibrium volume differs from the measured crystal volume by 0.6% in α-r-B_{12} and by 2.4% in α-t-B_{50}. Our calculation shows that at the calculated equilibrium volume, α-t-B_{50} is lower in energy than α-r-B_{12} by about 1.21 eV per atom, which seems to be large. Because of the structural complexity of α-t-B_{50}, which has a

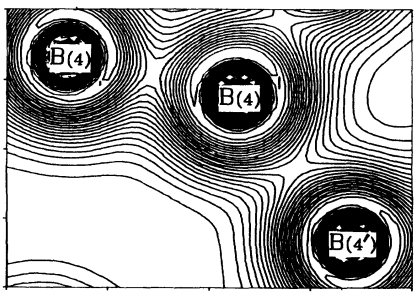

FIG. 13. Charge-density contour in α-t-B_{50} in a plane containing B(4)-B(4)-B(4)′ atoms [see Fig. 2(b)]. The units of the contour are the same as in Fig. 4.

large unit cell with boron atoms in different types of bonding, and also the metallic nature of the band, it is much more difficult to have accurate total-energy data for α-t-B_{50} than for α-r-B_{12}. This difficulty is already reflected in the larger fitting error in α-t-B_{50} mentioned in Sec. III and in the greater deviation of the equilibrium volume from the crystal data. For this reason, the relative stability of α-r-B_{12} and the α-t-B_{50} predicted by our calculation should be treated with caution. Nevertheless, in the following discussion, we have to assume a similar level of accuracy in the total energies for the two crystals with the caveat of possible numerical problems with the α-t-B_{50} phase. We are not aware of any other published calculation on the total energy of α-t-B_{50}.

The converted curves for pressure versus volume are shown in Fig. 14(b). The linear curves give a slope of -2.33 and -3.25 Mbar for α-r-B_{12} and α-t-B_{50}, respectively. Our calculated equilibrium volumes, the bulk modulus, the pressure coefficients, and the cohesive energies for α-r-B_{12} and α-t-B_{50} are summarized in Table II. As expected, the bulk modulus is large, consistent with its mechanical hardness. α-t-B_{50} has a larger bulk modulus than α-r-B_{12}. Also listed are the available experimental data and the results of other recent calculations. The experimental cohesive energies cited are believed to be only approximate values measured for unspecified structures of boron (Refs. 32 and 33). Our results on α-r-B_{12} agree well with other recent local-density total-energy calculations.[7,8] Since we believe we have obtained a similar level of accuracy in total energy for α-t-B_{50} as in α-r-B_{12}, it is possible that the former is thermodynamically more stable at zero temperature. As pressure is increased, our calculation predicts a possible structural phase transition from α-t-B_{50} to α-r-B_{12} at a volume of about 3.4 Å^3 per B atom, or at a pressure of about 360 GPa. However, at such a high pressure, it is likely that the structures of both phases may be significantly changed, and our calculation may not correspond to a real physical situation. Mailhiot, Grant, and McMahan,[8] in their local-density total-energy calculation, predicted that α-r-B_{12} may transform into a body-centered-tetragonal structure at a pressure of 210 GPa, and then to a face-centered-cubic structure at a pressure of 360 GPa.

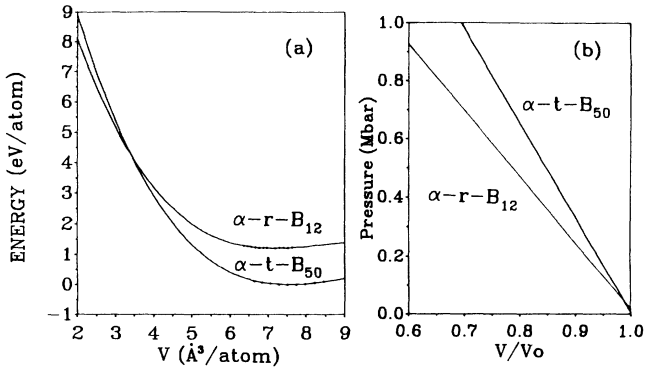

FIG. 14. (a) Calculated total energy of α-r-B_{12} and α-t-B_{50} as a function of volume. (b) Calculated pressure vs volume.

We have not investigated the energetics of other possible phases for boron in this paper.

VII. OPTICAL PROPERTIES

The calculated interband optical conductivity σ for α-r-B_{12} for photon energy up to 40 eV is shown in Fig. 15(a). The calculated absorption threshold is 2.18 eV, which corresponds to the direct band gap of 2.17 eV at Γ. The absorption rises quickly about the direct-gap threshold. In the low-energy region, the major structures in the calculated $\sigma(\omega)$ curve are at 4.8, 6.8, and 7.8 eV with sharp minima at 5.0, 7.42, and 12.3 eV. From 12.0 eV up, there are many more structures and the σ curve steadily decreases.

We find only one recent optical-absorption measurement on α-r-B_{12} near the absorption threshold.[34] The measured data are compared with the calculation in the inset of Fig. 15(b). Although specific agreement in the structure has not been achieved, there is no doubt that the general shapes of the absorption spectrum in this range are in quite good agreement.

The imaginary part of the dielectric function $\epsilon_2(\omega)$ can be obtained from the $\sigma(\omega)$ curve and the real part $\epsilon_1(\omega)$ can be obtained from Kramers-Kronig conversion. The $\epsilon_1(\omega)$ and $\epsilon_2(\omega)$ curves thus obtained are shown in Figs. 15(b) and 15(c), respectively. We have obtained a zero-frequency value of 7.7 for $\epsilon_1(0)$, which is close to the re-

TABLE II. Calculated total-energy data for α-rhombohedral B_{12} and α-tetragonal B_{50}.

	α-r-B_{12}			α-t-B_{50}
	This work	Other calc.	Expt.	This work
E (a.u./B atom)	−2.8148			−2.8591
V_{min}/V_{expt}	0.994			0.976
B (mbar)	2.45	2.49[a]		3.51
		2.66[a]		
B′	0.60			−11.46
E_{coh} (eV)	6.21	6.84[b]	5.9[c]	8.39
		7.4[a]	5.77[d]	
		7.0[a]		

[a]Reference 8.
[b]Reference 7.
[c]Reference 32.
[d]Reference 33.

cently reported value of 6.[35] The calculated energy-loss function for α-r-B_{12} is shown in Fig. 15(d). The bulk-plasmon excitation is at a fairly high energy, namely between 28 and 34 eV with the peak centered around 31.0 eV.

The calculation for the optical properties for α-t-B_{50} crystal is far more difficult because of the large unit cell and huge number of band states involved. We have limited our calculation of optical conductivity to a frequency range of only 10.0 eV. Because α-t-B_{50} is shown to be metallic, there would probably be Drude-like intraband transitions in the far-infrared frequency region, which is not accounted for by the present interband calculation.

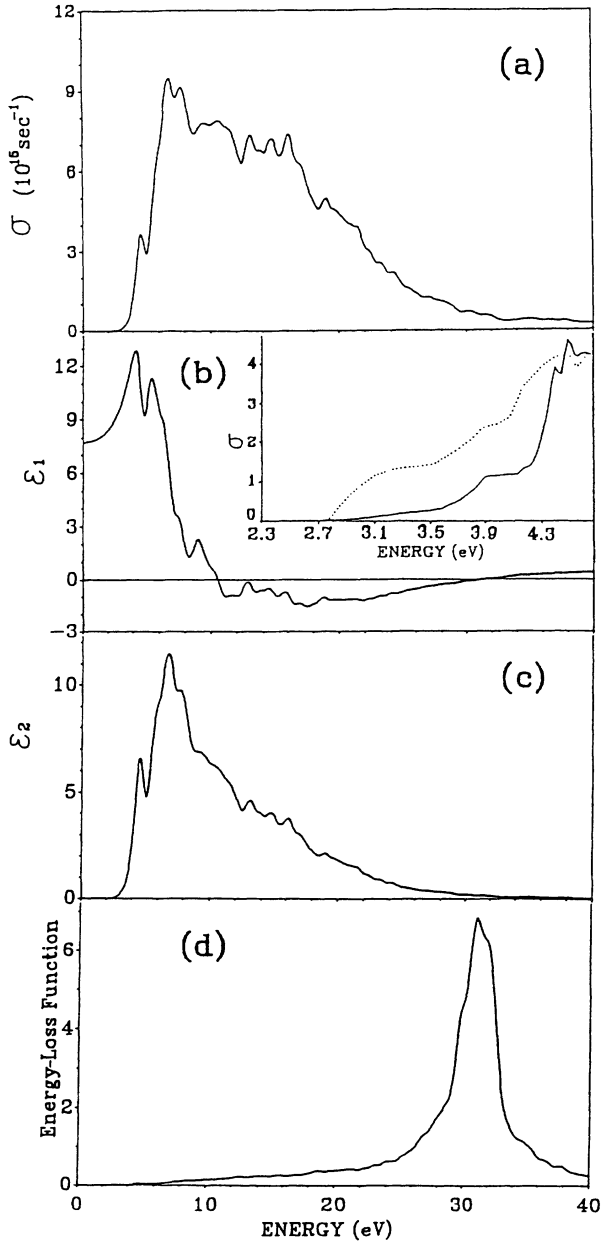

FIG. 15. Optical properties of α-r-B_{12}: (a) σ; (b) ϵ_1; (c) ϵ_2; (d) ELF. Inset in (a) σ near threshold compared to the measured absorption of Ref. 34.

However, the empty hole states near the top of the VB are likely to be highly correlated. Whether a free-electron-like Drude model of optical transition is applicable in this range is a matter of conjecture. The calculated interband optical conductivity σ, the real and imaginary parts of dielectric function, and the energy-loss function are displayed in Figs. 16(a)–16(d). The optical spectra for α-t-B_{50} are very different from the semiconducting α-r-B_{12}. Ignoring the results below 0.4 eV where intraband transitions dominate, the σ curve shows a strong peak at 1.1 and 1.5 eV and reaches a minimum at 1.8 eV. Beyond 2.0 eV, σ steadily increases until it reaches 5.6 eV, and then the absorption increases very rapidly, reaching a major peak at 7.7 eV and a valley at 10.0 eV. There are many small structures in the 6–10-eV range, similar to the case of α-r-B_{12}. It is clear that the absorption structures below 2 eV come from the transitions from the occupied states to the empty intrinsic hole

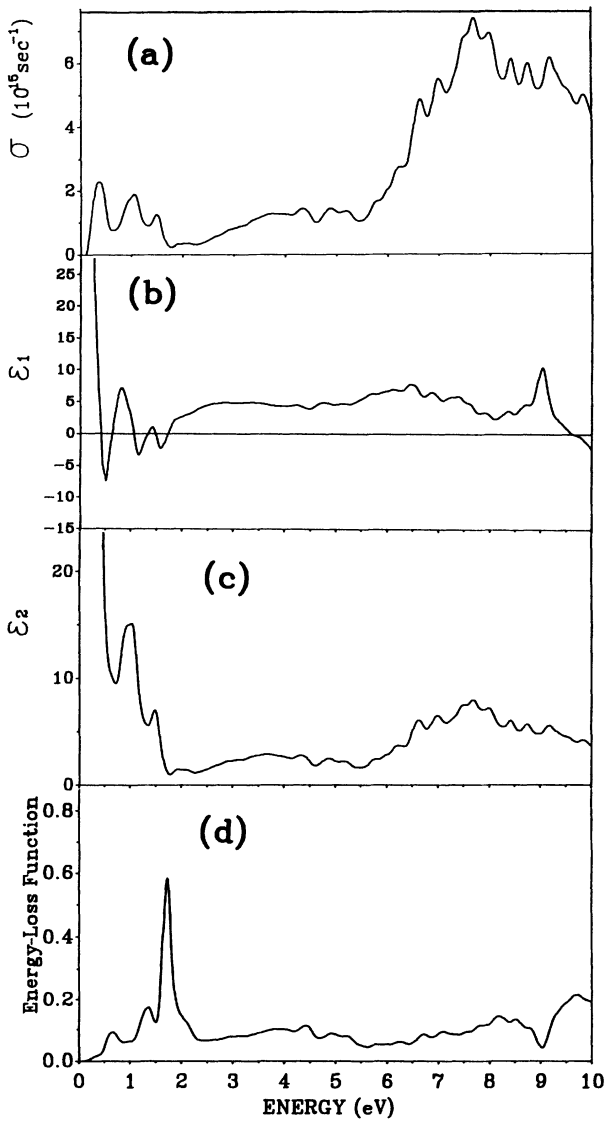

FIG. 16. Optical properties of α-t-B_{50}: (a) σ; (b) ϵ_1; (c) ϵ_2; (d) ELF.

states discussed earlier. The low absorption in the 2.0–5.5-eV range is most likely due to the presence of the semiconductorlike band gap. Above 5.5 eV, the optical transitions are all from below the Fermi level to the upper CB above the gap states and the spectrum starts to resemble that of α-r-B_{12}. The ELF shows a sharp structure at 1.8 eV. It is possible that bulk-plasmon excitation at a higher frequency than 30.0 eV may be present in α-t-B_{50}. We are not aware of any experimental measurements on the optical properties of α-t-B_{50}.

VIII. SUMMARY AND CONCLUSIONS

We have studied the electronic and the optical properties of α-r-B_{12} and α-t-B_{50} crystals using a first-principles method. The results obtained are in good agreement with the available experimental data and some other recent calculations. α-r-B_{12} is shown to be a semiconductor with an indirect band gap, while α-t-B_{50} is a metal with a semiconductorlike band structure. It is pointed out that the bonding structure in boron crystals in which the essential structural unit is an icosahedron cluster is very complicated and cannot be interpreted on the basis of simple molecular-orbital calculation. The total-energy calculation predicts α-t-B_{50} to be more stable than α-r-B_{12} at zero temperature, but a structural transformation may take place at a high pressure. The optical-properties calculation shows vastly different results for α-r-B_{12} and α-t-B_{50}, largely because of their fundamental difference in band structures. A bulk-plasmon excitation at 31 eV is predicted for α-r-B_{12} while the ELF for α-t-B_{50} has a sharp structure at 1.8 eV.

Emin proposed that electrical transport in B crystals is due to small polarons and the formation of bipolaron states may lead to a superconducting state in boron or boron-rich compounds.[1] We have already pointed out the resemblance between the band structures of α-t-B_{50} and of the $YBa_2Cu_3O_7$ superconductor. We may further point out the structural similarities in the B icosahedron with C_{60}, which is a truncated icosahedron with the same point-group symmetry. C_{60} forms a fcc lattice with the icosahedron C_{60} units as the building block.[36] Unlike the B compounds, the bonding between C_{60} clusters in forming a crystal lattice is of the weak van der Waal type instead of the much stronger covalent type of bonding in B crystals; and with very different optical properties.[37] But when intercalated with an alkali-metal element such as K or Rb, superconductivity with T_c as high as 28 K has been demonstrated.[38,39] Because of these similarities between the boron crystals and the novel superconductors, it is of high interest to investigate if superconductivity is a real possibility in some of the B or B-rich compounds. Since the understanding of the electronic structure of a material is the first step towards such a direction, it is our intention to extend the present calculation to other B-rich crystals such as $B_{12}C_3$, $B_{12}P_2$, and $B_{12}As_2$, etc.

ACKNOWLEDGMENT

This work is supported by the U.S. Department of Energy under Grant No. DE-FG02-84ER45170.

[1] D. Emin, Phys. Today **40** (1), 55 (1987); see also *Boron Rich Solids,* edited by D. Emin, T. L. Aselage, and C. L. Beckel, AIP Conf. Proc. No. 140 (AIP, New York, 1986).
[2] J. L. Hoard and R. E. Hughes, in *The Chemistry of Boron and Its Compounds,* edited by E. L. Muetterties (Wiley, New York, 1967), p. 25.
[3] F. Perrot, Phys. Rev. B **23**, 2004 (1981).
[4] D. M. Bullett, J. Phys. C **15**, 415 (1982).
[5] A. C. Switendick, in *Novel Refractory Semiconductors,* edited by D. Emin, T. L. Aselage, and C. Wood, Materials Research Society Symposia Proceedings No. 97 (MRS, Pittsburgh, 1987), p. 45.
[6] S. Lee, D. M. Bylander, and L. Kleinman, Phys. Rev. B **42**, 1316 (1990).
[7] D. M. Bylander, L. Kleinman, and S. Lee, Phys. Rev. B **42**, 1400 (1990).
[8] C. Mailhiot, J. B. Grant, and A. K. McMahan, Phys. Rev. B **42**, 9033 (1990).
[9] A. C. Switendick and B. Morosin (unpublished).
[10] L. V. McCarty, J. S. Kasper, F. N. Horn, B. F. Decker, and A. E. Newkirk, J. Am. Chem. Soc. **80**, 4507 (1958).
[11] B. F. Decker and J. S. Kasper, Acta Crystallogr. **12**, 503 (1959).
[12] A. W. Laubengayer, D. T. Hurd, A. E. Newkirk, and J. L. Hoard, J. Am. Chem. Soc. **65**, 1924 (1943).
[13] J. L. Hoard, S. Geller, and R. E. Hughes, J. Am. Chem. Soc. **73**, 1892 (1951).
[14] J. L. Hoard, R. E. Hughes, and D. E. Sands, J. Am. Chem. Soc. **80**, 4507 (1958).
[15] R. E. Hughes *et al.*, J. Amer. Chem. Soc. **85**, 361 (1963).
[16] J. L. Hoard, D. B. Sullenger, C. H. Kennard, and R. E. Hughes, J. Solid State Chem. **1**, 216 (1970).
[17] M. Vlasse, R. Naslain, J. S. Kasper, and K. Ploog, J. Solid State Chem. **28**, 289 (1979).
[18] L. Gorski, Phys. Status Solidi **3**(9), K317 (1963); 289 (1979).
[19] W. Y. Ching, J. Am. Ceram. Soc. **73**, 3135 (1990).
[20] F. D. Murnaghan, Proc. Natl. Acad. Sci. USA **30**, 244 (1944).
[21] F. H. Horn, J. Appl. Phys. **30**, 1611 (1959).
[22] O. A. Golikova, Phys. Status Solidi A **86**, K51 (1984).
[23] B. Morosin, A. W. Mullendore, D. Emin, and G. A. Slack, in Ref. 1, p. 70 (1986).
[24] H. C. Longuet-Higgins and M. de V. Roberts, Proc. R. Soc. London **230A**, 110 (1955).
[25] W. Y. Ching, Y.-N. Xu, G. L. Zhao, K. W. Wong, and F. Zandiehnadem, Phys. Rev. Lett. **59**, 1333 (1987).
[26] G.-L. Zhao, Y.-N. Xu, W. Y. Ching, and K. W. Wong, Phys. Rev. B **36**, 7203 (1987).
[27] K. Ploog, H. Schmidt, E. Amberger, G. Will, and K. H. Kossubutzki, J. Less Common Met. **29**, 161 (1972).
[28] G. Will and K. H. Kossubutzki, J. Less Common Met. **47**, 33 (1976).
[29] W. Y. Ching and B. N. Harmon, Phys. Rev. B **34**, 5305 (1986).
[30] F. Zandiehnadem and W. Y. Ching, Phys. Rev. B **41**, 493 (1990).
[31] Y.-N. Xu and W. Y. Ching, Phys. Rev. B **44**, 7787 (1991).
[32] C. Kittle, *Introduction to Solid State Physics,* 6th ed. (Wiley,

New York, 1986), p. 55.
[33]R. Hultgren *et al.*, in *Selected Values of the Thermodynamic Properties of the Elements* (American Society of Metals, Metal Park, Ohio, 1973), p. 55.
[34]H. Werheit, U. Kuhlman, N. E. Solov'er, G. P. TsisKarishvili, and G. Tsagareishvili, in the *10th International Symposium on Boron, Borides and Related Compounds,* edited by D. Emin, T. L. Aselage, A. C. Switendick, B. Morosin, and C. L. Beckel (AIP, New York, 1991), p. 350.
[35]G. A. Samar, H. L. Tardy, E. L. Venturini, T. L. Aselage, and D. Emin, Bull. Am. Phys. Soc. **36**, (3), 780 (1991).
[36]R. M. Fleming *et al.*, Materials Research Society Symposium Proceedings No. 206 (MRS, Pittsburgh, 1991), p. 691.
[37]W. Y. Ching, M.-Z. Haung, Y.-N. Xu, W. G. Harter, and F. T. Chan, Phys. Rev. Lett. **67**, 2045 (1991).
[38]A. F. Hebard *et al.*, Nature **350**, 600 (1991).
[39]M. J. Rosseinsky *et al.*, Phys. Rev. Lett. **66**, 2830 (1991).